Neuropharmacology 287 (2026) 110830

Contents lists available at ScienceDirect

Neuropharmacology

journal homepage: www.elsevier.com/locate/neuropharm

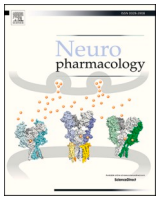

# Nose-to-brain delivery of dopamine to the striatum of rats using neurotransmitter-loaded solid lipid nanoparticles: an *in vivo* study by brain microdialysis

Laura Dazzi [a,1], Giuseppe Talani [b,1], Giuseppe Trapani [c], Luigi Capasso [c], Annalucia Carbone [d], Sante Di Gioia [d], Massimo Conese [d], Adriana Trapani [c,**], Enrico Sanna [a,b,*]

[a] Department of Life and Environmental Sciences, Section of Neuroscience and Anthropology, University of Cagliari, S.P. 8, km 0,70, Monserrato, 09042, Italy
[b] Institute of Neuroscience, National Research Council (CNR), Cittadella Universitaria di Monserrato, S.P. 8, km 0,700, Monserrato, 09042, (CA), Italy
[c] Department of Pharmacy-Drug Sciences, University of Bari "Aldo Moro", 70125, Bari, Italy
[d] Department of Clinical and Experimental Medicine, University of Foggia, 71122, Foggia, Italy

ARTICLE INFO

*Keywords:*
Solid lipid nanoparticles
Intranasal administration
Microdialysis
Electrophysiological experiments
Striatal projection neurons
HCN channels
$I_h$ currents

ABSTRACT

The intranasal route is a noninvasive method of delivering therapeutic compounds to the Central Nervous System (CNS). However, challenges associated with this method include reduced drug absorption, limited administered volume, insufficient nasal permeability, and enzymatic nasal metabolism. Nanotechnology-based delivery systems are being developed to overcome these limitations and improve drug availability and therapeutic effectiveness. In this regard, we recently developed dopamine (DA)-loaded solid lipid nanoparticles (DA-SLNs) using self-emulsifying Gelucire® 50/13 to form PEGylated SLNs for intranasal administration. To enhance mucoadhesion, we coated these lipid nanoparticles with the mucoadhesive cationic polymer glycolchitosan (GCS). In the present study, we performed microdialysis and electrophysiological experiments in a male rat model to evaluate the ability of GCS-DA-SLNs, when administered intranasally, to modify striatal extracellular DA concentrations and induce changes in the functional properties of striatal neurons. The results showed that intranasal administration of GCS-DA-SLNs at DA doses of 2.5 and 4 mg/kg significantly increased the extracellular concentration of DA (+130 ± 38 %) and the extracellular concentration of DOPAC (only at the lower dose of 1 mg/kg, by 70 ± 3 %). Ex vivo electrophysiological recordings in striatal neurons revealed that intranasal administration of GCS-DA-SLNs, at a DA dose of 4 mg/kg, but not 2.5, mg/kg, enhanced HCN-mediated $I_h$ current amplitude. A similar effect was also observed *in vitro* when striatal neurons were exposed to DA or the D1 receptor agonist SKF81297. Overall, our data underscore the significant potential of using GCS-DA-SLN nanocarriers to efficiently deliver DA and other therapeutic compounds via the nose-to-brain pathway.

## 1. Introduction

Neurodegenerative diseases are chronic, progressive, and debilitating multifactorial age-related neurological conditions that are characterized by nerve cell loss and impairments in brain function.

Among neurological disorders, Parkinson's disease (PD) is the second most prevalent neurodegenerative pathology in developed countries, following Alzheimer's disease. Its incidence is approximately 3 % in the population aged up to 65 years, rising to 5 % for those over 85 (Cerri et al., 2019). PD patients typically present impairments in body movements, including tremor, bradykinesia, rigidity, and postural instability. Additionally, non-motor symptoms including anxiety and depression, insomnia, gastrointestinal disturbances, and olfactory and visual changes are also frequently observed (Hayes, 2019). The primary pathophysiological features of PD are the loss of dopaminergic neurons in the substantia nigra pars compacta, accompanied by a consequent reduction in dopamine (DA) levels in the striatum (Muddapu and Chakravarthy, 2021).

* Corresponding author. Department of Life and Environmental Sciences, Section of Neuroscience and Anthropology, University of Cagliari, S.P. 8, km 0,700, 09042 Monserrato, Italy.
** Corresponding author.
*E-mail addresses:* adriana.trapani@uniba.it (A. Trapani), esanna@unica.it (E. Sanna).
[1] Laura Dazzi and Giuseppe Talani contributed equally to this work.

https://doi.org/10.1016/j.neuropharm.2026.110830
Received 25 June 2025; Received in revised form 29 December 2025; Accepted 1 January 2026
Available online 2 January 2026

The standard treatment for PD symptom management is focused on restoring normal DA levels. This approach aims at compensating for the loss of dopaminergic neurons and the resulting DA deficiency by replenishing its content to functional levels. However, DA per se is unable to cross the BBB due to its physicochemical properties and has a marked susceptibility to metabolic degradation (Chemuturi et al., 2006; Di Gioia et al., 2015). To overcome these problems, the DA precursor L-Dopa is clinically employed, which is capable of cross the BBB via the L-AA transporter and is converted to DA in the brain by L-Dopa decarboxylase.

One promising strategy to overcome the challenge posed by the BBB in neurodegenerative disorders is the use of intranasal administration. This non-invasive drug delivery route is characterized by rapid absorption, high patient compliance, and the ability to bypass the blood-brain barrier (BBB). These features make it especially attractive for central nervous system (CNS) therapies and emergency situations. The nasal cavity's rich vascularization and large surface area facilitate a fast onset of action and prevent first-pass hepatic metabolism. This results in higher bioavailability for many drugs compared to oral or parenteral routes, as well as potentially reduced systemic side effects. This route is particularly advantageous for potent, low-molecular-weight, and lipophilic drugs. It is being explored more and more for treating CNS disorders, managing pain, administering hormone therapies, and treating acute seizures (Crowe and Hsu, 2022; Erdo et al., 2018; Keller et al., 2022; Lofts et al., 2022).

In this context, de Souza Silva et al. first demonstrated, by *in vivo* microdialysis, that intranasal administration of drugs active on the dopaminergic system, including the psychostimulants cocaine and amphetamine, and the anti-PD drug L-Dopa, can increase extracellular levels of DA in the striatum (De Souza Silva et al., 1997). Further studies have examined the behavioral effects of intranasal administration of DA and L-Dopa (Buddenberg et al., 2008; de Souza Silva et al., 2008), including their efficacy in relieving parkinsonian symptoms in an animal model of PD consisting of rats injured at the level of the nigrostriatal pathway with 6-hydroxy-dopamine (6-OH-DA) (Chao et al., 2012; Pum et al., 2009).

The intranasal route represents a non-invasive method for delivering many therapeutic agents (including those that are poorly lipophilic) directly to CNS. The results of autoradiographic studies with $^{3}$H-DA have demonstrated that the neurotransmitter is transferred into the olfactory bulb after intranasal administration, achieving rapid access to the brain (Dahlin et al., 2000). The central transport of DA is mediated by specific transporters, primarily the large neutral amino acid transporter (LAT), which facilitates the transfer of DA-related molecules to the brain, including L-Dopa and other DA-associated amino acids (Uchino et al., 2002). Interestingly, at the level of the nasal mucosa, the active presence of the DA transporter (DAT) and organic cation transporter 2 (OCT-2) has been demonstrated (Chemuturi and Donovan, 2006).

Although intranasal administration provides direct drug access to the brain, it faces obstacles including limited drug absorption, limited administration dose, insufficient nasal permeability, presence of nasal enzymatic barriers and so on. These limitations underscore the need for advanced nanotechnology-based delivery systems to enhance drug availability and therapeutic efficacy (Rehman et al., 2019).

The various polymer- and lipid-based nanoformulations have unique and easily tailored properties, making them a potential carrier for drug delivery to the brain (Saha et al., 2023; Zheng et al., 2024). These nanocarriers can protect the drug from enzymatic degradation to facilitate their transport across the nasal mucosa to the brain. They also provide greater adhesion to the mucosal surface, ensuring a higher concentration of drug at the site of action. Increased drug loading, controlled release, improved absorption and mucoadhesiveness, enhanced stability, biocompatibility and biodegradability are some of the features of nanocarriers that are essential for drug delivery to the brain. On the whole, such nanoformulations can considerably enhance the therapeutic efficacy while minimizing undesired drug side effects (Bourganis et al., 2018; Gandhi et al., 2024). A further relevant limitation occurring when drugs are administered via the nose is that the movement of mucus lowers their residence time with the nasal mucosa and this problem is referred to as mucociliary clearance. To satisfactorily overcome this issue, a most followed approach involves the coating of the nanoformulations with mucoadhesive polymers enhancing the residence time of drug in the nasal cavity (Gandhi et al., 2024).

Recently, lipid nanoparticles, specifically DA-loaded solid lipid nanoparticles (DA-SLNs), were developed by us by employing the self-emulsifying Gelucire® 50/13 ((Stearoyl macrogol-32-glycerides) as lipid matrix (Cometa et al., 2020). These last lipid nanocarriers, which actually constitute PEGylated SLNs, have been investigated for encapsulation not only of lipophilic drugs but also of hydrophilic ones (Castellani et al., 2024; Trapani et al., 2021b). Such lipid nanoparticles can be usefully coated with a mucoadhesive cationic polymer as chitosan (CS) or its derivative to give a positive surface charge to these nanoparticles enabling, so, a strong electrostatic interaction with the negatively charged glycoprotein mucin chains due to the sialic acid and sulphate groups present (Palazzo et al., 2017). For this purpose, we selected a CS derivative such as glycol chitosan (GCS) as coating of the PEGylated SLNs since it is water soluble both at acidic and neutral pH values, unlike the parent CS which is water soluble at acidic pH only. Moreover, we showed that GCS is endowed with inhibition properties of the efflux pumps P-glycoprotein (P-gp) which reduces the amount of drug in the brain (Keller et al., 2022; Trapani et al., 2014).

*In vitro* physicochemical characterization indicates that these nanoparticles may be suitable for brain delivery of DA following intranasal administration. Indeed, SLNs were capable of encapsulating DA (DA-SLNs) with an efficiency of approximately 80 % and were additionally coated with the mucoadhesive polysaccharide GCS (GCS-DA-SLNs). Furthermore, *in vitro* studies demonstrated that GCS-DA-SLNs were able to release DA continuously at a rate of 9 % over a 48-h period (Trapani et al., 2021a). The main goal of this study was to assess the efficacy of intranasally administered GCS-DA-SLNs in transferring DA to the brain, with a particular focus on the striatum, a region of the brain associated with motor symptoms of PD. Microdialysis and electrophysiological experiments were performed to investigate the ability of intranasally administered GCS-DA-SLNs to modify extracellular DA concentrations in the striatum and the resulting changes in the functional properties of striatal projection neurons (SPNs) in the dorsal striatum.

## 2. Materials and methods

### 2.1. Materials

Dopamine hydrochloride, Glycol chitosan (GCS, MW 400 kDa according to supplier instructions) and Tween® 85 were purchased from Sigma-Aldrich (Milan, Italy). Gelucire® 50/13 (solid pellets of Stearoyl polyoxyl-32 glycerides) was kindly donated by Gattefossè (France). For solutions and suspensions preparation, double distilled water was used. All other chemicals were of reagent grade. Esterase enzyme (carboxyl ester hydrolase, E.C. 3.1.1.1, corresponding to 15 units/mg solid) from porcine liver and porcine stomach mucin (type II, bound sialic acid about 1 %) was purchased from Sigma-Aldrich (Milan, Italy).

### 2.2. Solid lipid nanoparticle preparation

Following the melt homogenization method, DA-loaded Gelucire® 50/13 SLNs (DA-SLNs, SLN 1) and GCS coated DA-loaded Gelucire® 50/13 SLNs (GCS-DA-SLNs, SLN 2) were prepared as previously reported (Mallamaci et al., 2024; Trapani et al., 2021a). Briefly, 60 mg of the lipid Gelucire® 50/13 were melted at 70 °C and, in a separate vial, DA (10 mg), the surfactant (Tween® 85, 60 mg) and 1.37 mL diluted acetic acid, 0.01 %, w/v, were mixed and, then, heated at 70 °C. To obtain an emulsion, the resulting aqueous phase was added to the melted lipid phase at 70 °C and one cycle of homogenization was performed at

12300 rpm for 2 min with an UltraTurrax model T25 apparatus (Janke and Kunkel, Germany). Afterwards, the nanosuspension was cooled at room temperature and the resulting DA-SLNs, (SLN 1) centrifuged (16,000×*g*, 45 min, Eppendorf 5415D, Germany) and the obtained pellet was re-suspended in double distilled water for further studies.

To prepare the GCS-DA-SLNs (SLN 2), 1.37 g of a previously formed solution of GCS (5 mg/mL in AcOH 0.01, w/v) was added to the aqueous phase containing DA (10 mg) and the surfactant (Tween® 85, 60 mg) and, as above, mixed with lipid Gelucire® 50/13 to achieve a pre-emulsion. Working up as reported above for SLN 1 the required SLN 2 were obtained, showing an average volume of about 1.5 mL of the final nanosuspension. Control SLNs were either the ones without both DA and GCS (namely, plain SLNs) or the ones without DA, but containing GCS (namely, GCS-SLNs).

### 2.3. SLN physicochemical characterization

SLN particle size and polydispersity index (PDI) were acquired by ZetasizerNanoZS (ZEN 3600, Malvern, UK) apparatus according to photon correlation spectroscopy (PCS) mode. After dilution 1:1 (v:v) with double distilled water, the particle size and polydispersity index (PDI) of SLNs were measured. For evaluation of zeta-potential of SLNs, measurements were performed at 25 °C (ZetasizerNanoZS, ZEN 3600, Malvern, UK) after sample dilution 1:20 (v:v) with KCl (1 mM, pH 7) (Castellani et al., 2024).

For DA quantification in the SLNs, the enzymatic digestion of SLN pellets operated by esterases took place due. The enzyme esterase catalyzed the hydrolysis reaction of the glycerides belonging to the Gelucire® 50/13. Firstly, by dissolving the enzyme at 12 I.U./mL in phosphate buffer (pH 5) 1–2 mg of freeze-dried SLNs were incubated with 1 mL of the enzyme solution for 30 min in an agitated (40 rpm/min) water bath set at 37 °C (Julabo, Milan, Italy). Afterwards, the resulting mixture was centrifuged (16,000×*g*, 45 min, Eppendorf 5415D) and in the supernatant DA levels were determined according to the HPLC procedure previously described (De Giglio et al., 2023).

The encapsulation efficiency (E.E.%) was calculated by Eq. (1):

$$E.E.\% = \text{DA in the supernatant after esterase assay/Total DA} \quad \text{Eq. 1}$$

where total DA is intended as the starting amount of the neurotransmitter used for SLN preparation. For each type of SLNs, the study was performed in triplicate.

The mucoadhesive properties of DA-SLNs (SLN 1) and GCS-DA-SLNs (SLN 2) were assessed in Simulated Nasal Fluid (SNF) following the *in vitro* turbidimetric method (Cassano et al., 2020). SNF was prepared dissolving $CaCl_2$ $2H_2O$ (0.32 mg/mL), KCl (1.29 mg/mL) and NaCl (7.45 mg/mL) in water maintaining the pH value in the range 5–6. Briefly, to a freshly prepared mucin dispersion in SNF (1 mg/mL, 6 mL) kept in a water bath at 37 °C under stirring, freeze dried SLN formulations, previously dispersed in 6 mL of SNF, were added. The percentage of transmittance of these stirred mixtures was measured at 37 °C at predetermined times of incubation at the wavelength of 650 nm using a using a PerkinElmer Lambda Bio 20 spectrophotometer. All experiments were repeated in triplicate and the percentage of transmittance values are reported as mean ± standard deviation.

For visualization of SLN 1 and SLN 2, a cryogenic transmission electron microscopy (Cryo-TEM) apparatus was adopted as already reported (Trapani et al., 2021b). For sample preparation, the copper grids were brought into contact with aqueous dispersions of the samples for 30 s, before the grids were treated with 2 % w/v phosphotungstic acid for 10 s before drying.

### 2.4. In vitro DA release from GCS-DA-SLNs in SNF

The *in vitro* release studies from GCS-DA-SLNs were carried out as previously described (Cometa et al., 2020). Briefly, a freshly prepared pellet of the particles was aliquoted in order to provide DA in the range of 1–1.2 mg. Simulated Nasal Fluid (SNF) was prepared as above mentioned. Then, 1.5 mL of SNFs were poured in Eppendorf tubes and *in vitro* release test started once to the above-mentioned aliquots of SLN pellet were added to each tube at 37 °C and 40 rpm/min. At predetermined time-points each of the Eppendorf tubes were centrifuged at 16,000×*g* for 45 min, and the DA concentrations were determined in the resulting supernatants by HPLC, as previously described (Cometa et al., 2020). All release experiments were carried out in triplicate.

The DA release data from GCS-DA-SLNs were fitted to some kinetic models including zero-order, Higuchi and Korsmeyer–Peppas models, to determine the best fitting kinetic model and, consequently, to infer the possible mechanism of DA kinetic release. The mathematical equations used to describe DA dissolution curves are the following: $M_t = M_0 + k\,t$ for zero order model, $M_t = k_H\,t^{1/2}$ for Higuchi model, and $F_t = M_t/M_\infty = k\ x\ t^n$ for Korsmeyer–Peppas equation where $F_t$ is the drug fraction released at time t, k the diffusional release constant, n the diffusional exponent.

### 2.5. Formulation dosing

The solid lipid nanoparticles (SLNs) used in the experiments were of two types: GCS coated DA-loaded SLNs (GCS-DA-SLNs) and empty GCS coated SLNs (GCS-LSN). GCS-DA-SLNs can capture DA with an efficiency of 19 ± 3 % and has a final size of 171 ± 6 nm (Cometa et al., 2020). The GCS-DA-SLNs and the empty GCS-SLNs were suspended in double-distilled water (pH = 5) under light protection to prevent autoxidation (Umek et al., 2018). This occurred just prior to the experiment to obtain final DA doses of 1.0, 2.5, and 4.0 mg/kg of body weight in a constant total volume of 30 μL. The concentration of nanoparticles is between 1.5 and 16 mg/120 μL.

### 2.6. Animals

The present study was conducted using male Sprague–Dawley rats, 60–80 days of age, procured from Envigo (S. Pietro al Natisone, Italy). The animals were maintained under standard conditions, with an artificial 12-h light/dark cycle (light on at 7:00 a.m.), a constant temperature of 22 ± 2 °C, and a relative humidity of 65 %. The animals always had free access to water and standard food. The animal care and handling procedures employed for the entire experimental period were reviewed by the Organism for Animal Care and Wellness of the University of Cagliari (OPBA-UniCA) and approved by the Italian Ministry of Health (authorization no. 509/2024-PR) in accordance with the guidelines. These guidelines are outlined in the European Communities Council Directives (2010/63/UE, October 20, 2010) and the Italian law (D.L. 26, March 04, 2014). The study was conducted in accordance with the three Rs principles, which advocate for the reduction of animal suffering and the minimization of the number of animals used in experimentation.

### 2.7. Microdialysis and intranasal administration

Rats were anesthetized with isoflurane, and a concentric dialysis probe was inserted at the level of the right striatum (A −1.3, ML +3.0, V −7.5 relative to the bregma), according to the Paxinos and Watson rat brain atlas (Paxinos and Watson, 2004). The probes were prepared in our lab using Hospal Dasco dialysis membrane with a cutoff of 5000 Da, with an active length of the dialysis membrane restricted to 4 mm. The probes had an *in vitro* recovery value for DA of 21 ± 3 % (mean ± SEM); all the probes with a recovery value outside of this range were not used and the absolute concentration of DA was not corrected for recovery values.

Experiments were performed 24 h after surgery to allow for full recovery from anesthesia and surgery. On the day of the experiment, Ringer's solution [3 mM KCl, 125 mM NaCl, 1.3 mM $CaCl_2$, 1 mM $MgCl_2$,

23 mM $NaHCO_3$, 1.5 mM potassium phosphate (pH 7.3)] was pumped through the dialysis probe at a constant rate of 2 μL/min. The dialyzed samples, enriched in the neurotransmitters present in the synaptic space that will pass inside the fiber by passive diffusion, were collected at regular intervals of 20 min and immediately analyzed for their DA and its metabolite 3,4-Dihydroxyphenylacetic acid (DOPAC) content by HPLC as previously described (Dazzi et al., 2002). Once at least three consecutive samples had been obtained in which the DA and DOPAC concentrations do not vary by more than 20 %, the average of these samples was considered as the baseline value to which subsequent samples were referred. At this time, the rats, still with fiber connected to the perfusion pump, were lightly anesthetized with isoflurane (2 % in oxygen) and placed in the supine position. Anesthesia, although not necessary, is recommended to allow for precise administration of the compound and to avoid sneezing (Turner et al., 2011). After the induction of anesthesia, the animal's respiratory rate was closely monitored. Intranasal administration was performed using a Hamilton glass micro syringe with a 2.5 cm long silicone tube (outer diameter 0.8 mm) attached to the needle. The small tube is soft, and its length allows the solution to be deposited at the level of the olfactory mucosa, located at the bottom of the nasal cavity. Three 5-μL aliquots were injected into each of the two nostrils (with a 60-s interval between administrations), for a total administered volume of 30 μL of the aqueous suspension of GCS-DA-SLNs or GCS-SLNs not carrying DA. The rats were kept in the supine position until they awakened (after less than 1 min). The rats were then returned to their cages for subsequent dialysate collection. Samples were collected every 20 min for up to 8 h after intranasal administration of nanoparticles.

### 2.8. Brain slices preparation

For the ex vivo electrophysiological experiments, rats were sacrificed 30 min after intranasal administration of GCS-DA-SLNs or vehicle, which was conducted as described in the previous paragraph. Coronal brain slices were prepared in accordance with the protocol previously described by Adermark et al. (2009). In brief, rats were deeply anesthetized with isoflurane vapor (4 %) and rapidly decapitated to extract the brain. The brain was then placed in ice-cold modified artificial cerebrospinal fluid (aCSF) containing (in mM): 220 sucrose, 2 KCl, 0.2 $CaCl_2$, 6 $MgSO_4$, 26 $NaHCO_3$, 1.3 $NaH_2PO_4$, and 10 D-glucose; the pH was set to 7.4 by the addition of 95 % $O_2$ and 5 % $CO_2$ through aeration. Brain slices (250 μm thick) containing the dorsal striatum were then sectioned with a vibratome (Laica, series 1000) and were allowed to equilibrate for a minimum of 40 min in standard artificial cerebrospinal fluid (aCSF) containing (in mM): 126 NaCl, 3 KCl, 2 $CaCl_2$, 1 $MgCl_2$, 26 $NaHCO_3$, 1.25 $NaH_2PO_4$, and 10 D-glucose (pH 7.4, adjusted by aeration with 95 % $O_2$ and 5 % $CO_2$) at a controlled temperature of 35 °C. Subsequently, the slices were incubated for a minimum of 1 h at room temperature. Thereafter, they were transferred to a recording chamber and continuously perfused with aCSF at a flow rate of approximately 2 ml/min. All recordings were carried out at room temperature (24 °C).

### 2.9. In-vitro and ex-vivo electrophysiological experiments

Whole-cell patch-clamp recordings from striatal projection neurons (SPNs) of the dorsal striatum were performed as previously described (Adermark et al., 2009). Our analysis included only SPNs that expressed $I_h$ and were sensitity to the HCN channel blocker ZD7288. Neurons were visualized using an infrared differential interference contrast microscope (Olympus). Recording microelectrodes were prepared from borosilicate capillaries (outer diameter, 1.5 mm; inner diameter, 0.86 mm; Sutter Instruments, Novato, CA, USA) with an internal filament using a Flaming Brown puller (model P-97, Molecular Devices, Novato, CA, USA). The resistance of the micropipettes ranged from 3.5 to 6.0 MΩ when filled with an internal solution containing (in mM): 135 potassium gluconate, 10 $MgCl_2$, 0.1 $CaCl_2$, 1 EGTA, 10 Hepes-KOH (pH 7.3), and 2 ATP (disodium salt), pH 7.3 adjusted with 1 mM KOH. The access resistance ranged from 15 to 30 MΩ and was monitored throughout all patch-clamp recordings by injection of 10 mV hyperpolarizing pulses. Series resistance was not compensated, and cells were excluded from a further analysis if access resistance changed by more than 20 % during the recording. After the whole-cell configuration was reached, the average neuronal membrane characteristics were a resting membrane potential of $-65.9 \pm 1.6$ mV and a membrane capacitance of $133.4 \pm 2.2$ pF ($n = 18$ SPNs).

To elicit the hyperpolarization-activated currents ($I_h$), voltage-clamp recordings were performed with incremental hyperpolarizing steps of 10 mV of the membrane from −65 to −115 mV. The amplitude of $I_h$ (average, $-58 \pm 16$ pA, $n = 18$ SPNs) was measured as the difference between the maximum membrane current value in response to every voltage step and the baseline holding current at the beginning of each voltage-step. $I_h$ amplitude was normalized to the membrane capacitance of each cell and values are expressed in pA/pF. Bath application of the HCN selective blocker ZD7288 (10 μM) suppressed $I_h$ confirming the nature of these currents (result not shown).

Recording of the different neurophysiological parameters usually started at least 10 min after the whole-cell configuration (membrane patch break-in) was reached. Membrane currents were recorded with the use of an Axopatch 200-B amplifier (Axon Instruments), filtered at 2 kHz, and digitized at 5 kHz. The pClamp 10.7 software (Molecular Devices) was used, which allowed us to measure and analyze various kinetic parameters of the neuronal membrane, membrane potential and currents. For *in vitro* drug perfusion experiments using different concentrations of DA and SKF81297, after a control period needed to have a stable baseline of $I_h$ currents, single DA concentrations were applied for 5 min each for $I_h$ evaluation, calculating the percent change in $I_h$ amplitude.

### 2.10. Statistical analysis

The data are presented as mean ± SEM and compared by two-way analysis of variance (ANOVA) and Sidak's post hoc test for electrophysiology results, and by two-way ANOVA for repeated measures and Bonferroni's post-hoc test for microdialysis data, with the use of GraphPad Prism 10 software. A p-value of less than 0.05 was considered statistically significant.

## 3. Results and discussion

### 3.1. SLN characteristics

Herein, we completed the characterization of both lipid nanocarriers examined [*i.e.,* DA-SLNs (SLN 1) and GCS-DA-SLNs (SLN 2)] as for their mucoadhesive properties and for the prevalent mechanism working in the neurotransmitter release kinetic from the SLN 2 delivery system. Both these features were not described in our previous report (Trapani et al., 2021a).

Previously, we have already shown that, with the exception of the unloaded GCS-SLNs, both DA-SLNs and GCS DA-SLNs were less than 200 nm as mean particle size, so being suitable for intranasal administration (Trapani et al., 2021a). Furthermore, the higher E.E.% obtained for GCS-DA-SLNs led us to test them (and the corresponding control GCS-SLNs) from a pharmacological viewpoint (Trapani et al., 2021a).

As shown in Fig. 1, GCS-DA-SLNs (SLN 2) exhibited the most relevant reduction decrease in transmittance after 7 h of incubation time, resulting in a statistically significant difference compared with the control ($p < 0.001$ vs. HEC, respectively), suggesting high mucoadhesive properties for this nanostructured formulation.

Moreover, from a morphological point of view, TEM microphotographs previously showed (Trapani et al., 2021b) suggest that SLN 1 were characterized by compact round shape, while SLN 2 were endowed with slightly distorted round form.

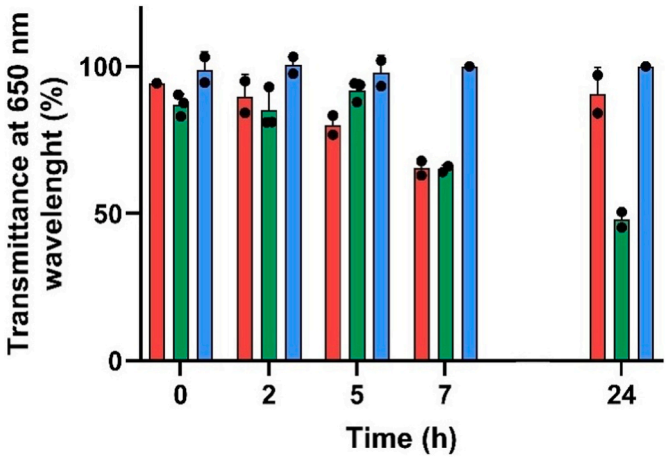


**Fig. 1.** Panel (A): Mucoadhesive properties in Simulated Nasal Fluid (SNF) of DA-SLNs (SLN 1) (red bars), GCS-DA-SLNs (SLN 2) (green bars) and hydroxyethylcellulose (HEC, blue bars) taken as positive control. The decrease of percentage of transmittance of SLN 1 and, particularly, SLN 2 (red and green bars, respectively) measured at 37 °C at predetermined times of incubation is due to nanocarrier-mucin aggregates formation (Cassano et al., 2020). Hence, such nanocarriers are characterized by better mucoadhesive properties of the positive control (HEC, blue bars) which is a recognized mucoadhesive polymer.

In addition, at 4 °C SLNs 2 have been already seen to be promising in terms of storage stability over the time, since their mean diameter and DA level could be maintained almost constant for two weeks (Trapani et al., 2021b).

Now, kinetic evaluation of DA release profile from GCS-DA-SLNs (SLN 2) was carried out to obtain some insight about the prevalent mechanism underlying the neurotransmitter release from the SLN 2 delivery system. Release data were fitted into the most followed release kinetic models including zero order, Higuchi and Korsmeyer–Peppas models and the best one should be that with the higher correlation coefficient ($R^2$). On this basis, the best fitted model should be the Higuchi release kinetic mode since the corresponding $R^2$ value was 0.9698, while the goodness of fit with Korsmeyer-Peppas and zero order models was lower ($R^2$ values of 0.8410 and 0.8999, respectively).

Higuchi describes drug release as a diffusion process based on the Fick's law leading to a square root time dependence and in Fig. 2 the DA release in function of time (panel A) and square root time (panel B) are shown. The Higuchi release kinetic model is characteristic of sustained delivery systems. Besides, it can be also stated that the initial burst release observed during the first minutes (Fig. 2, panel A) can be due to the diffusion of drug present on the nanoparticle outer surface, and might provide a fast onset of action. Overall, such results are consistent with what reported in literature for SLN formulations (Mura et al., 2021; Trapani et al., 2015). In addition, GCS-DA-SLNs (SLN 2) was identified as the most interesting formulation for nose-to-brain DA delivery offering some advantages as high drug encapsulation efficiency, protection from degradation, good mucoadhesive properties and sustained release worthy of further *in vivo* investigation.

### 3.2. Microdialysis experiments

Basal extracellular concentration of DA in the striatum (not corrected for probe recovery) was 15.7 ± 0.74 fmol/sample. Samples were collected for 8 h post-administration, but in Fig. 3 only the first 2 h were shown as after this period no significant changes in extracellular DA or DOPAC content were observed. Intranasal administration of GCS-DA-SLNs (1, 2.5 and 4 mg/kg) induced a dose-dependent increase in striatal DA extracellular concentration (Fig. 3A) with a maximal increase (+130 ± 38 % with respect to basal values) 20 min after administration of the higher dose that lasted for 80 min after administration. The lower dose (1 mg/kg) or of the empty SLN failed to significantly modify basal DA concentration. Two-way ANOVA revealed a significant effect of treatment [$F(2.894,46.31) = 5.023$, $p = 0.0047$], a significant effect of time [$F(3,16) = 7.821$, $p = 0.0019$], and a not significant interaction between factors [$F(18,96) = 1.385$, $p = 0.1568$].

On the contrary, intranasal administration of GCS-DA-SLNs induced an increase (+70 ± 3 %) in extracellular concentration of DOPAC only at the lower dose of 1 mg/kg, while the higher dose did not significantly modify this parameter (Fig. 3B). Two-way ANOVA revealed a significant effect of treatment [$F(3,12) = 3.783$, $p = 0.0404$], a not significant effect of time [$F(1.813,21.75) = 2.255$, $p = 0.1326$], and a significant interaction between factors [$F(18,72) = 1.855$, $p = 0.0344$].

Fig. 3C shows the DOPAC/DA ratio, as an index of DA metabolism. The ratio is 1.9 for the dose of 4 mg/kg, 5.03 for the dose of 2.5 mg/kg, and 1.6 for the dose of 1 mg/kg, with a statistically significant effect observed only for the intermediate dose of GCS-DA-SLNs.

Our results are in agreement with those obtained by De Souza Silva et al. (De Souza Silva et al., 1997) who demonstrated an increase in striatal DA concentration following the intranasal administration of cocaine, amphetamine or L-DOPA. In their paper, De Souza Silva et al. found that cocaine and amphetamine induced a dramatic increase in striatal extracellular DA concentration and a decrease in its metabolite, DOPAC, while L-DOPA increased both striatal DA (by about 30 % over basal values) and DOPAC (+20 % with respect to basal values). In our study, the administration of GCS-DA-SLNs produced an effect more similar to that induced by L-DOPA administration in the study by De Souza Silva et al., suggesting that GCS-DA-SLNs might increase DA levels without interfering with reuptake mechanisms, as occurs with cocaine or amphetamine.

Our present results do not provide evidence of the exact route travelled by GCS-DA-SLNs to deliver DA to the striatum. In fact, previous evidence suggests that substances administered intranasally can be absorbed by the nasal mucosa and enter the brain via neuronal or extraneuronal pathways (De Souza Silva et al., 1997). In the former case, drugs would enter the olfactory or trigeminal neurons by endocytosis

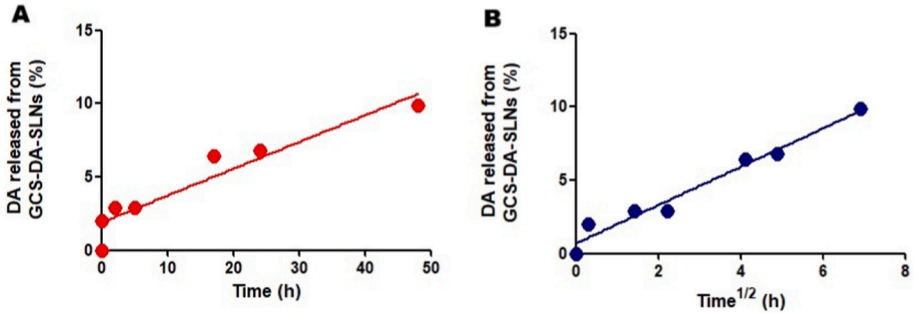


**Fig. 2.** Panel (A): DA released from GCS-DA-SLNs plotted in function of time. Panel (B): DA released from GCS-DA-SLNs plotted in function of square root of the time, as required by the Higuchi release kinetic.

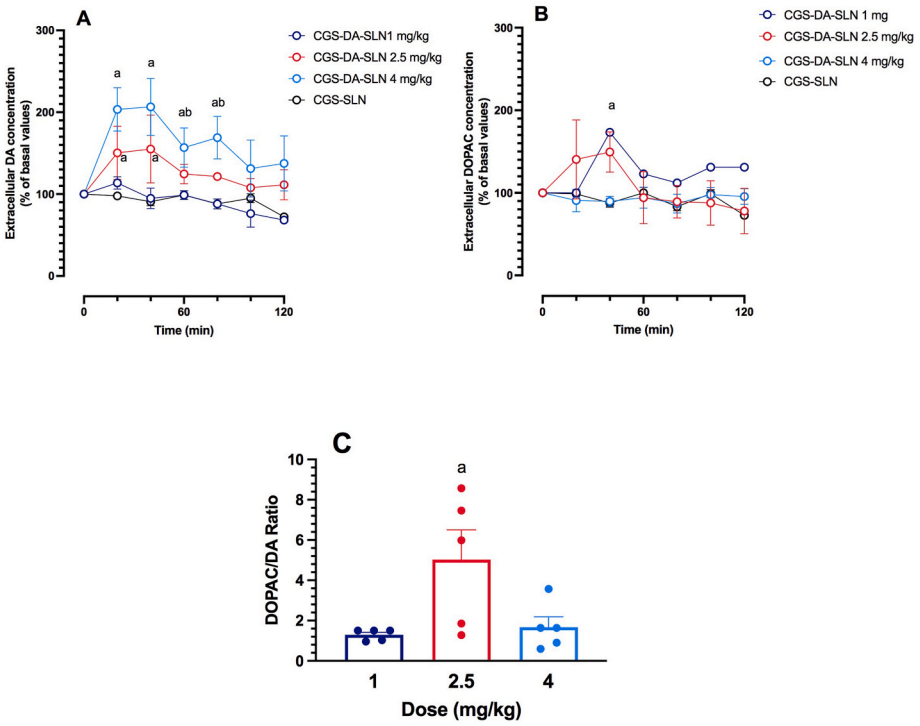


**Fig. 3.** Effect of intranasal administration of GCS-DA-SLNs or GCS-SLNs on extracellular concentration of DA, DOPAC, and the ratio DOPAC/DA in the striatum of rats. Twenty-four hours after surgical implantation of the microdialysis probe, basal DA (panel A) and DOPAC (Panel B) extracellular concentration and DOPAC/DA ratio (panel C) were measured in the striatum of rats. After reaching a stable basal concentration (see results for basal values), animals were lightly anesthetized with isoflurane and GCS-DA-SLNs (1, 2.5, or 4 mg/kg) or GCS-SLNs were intranasally administered. Rats rapidly woke up from anesthesia and were returned to their home cage where dialysis samples were collected every 20 min for 2 h.
DOPAC/DA ratio was calculated for the maximal effect (40 min after administration) induced by the 3 doses administered intranasally (1, 2.5, and 4 mg/kg).
Data represent mean ± SEM of 5 rats per group and are expressed as percentage of basal values.[a]P<0.01 vs basal values; [b]P < 0.01 vs correspondent time point of controls (GCS-SLNs).

and be transported through the axons into the brain were they are released by exocytosis (Crowe et al., 2018). This process has been described as slow, and it has been calculated that the time required to transport a substance the length of the olfactory neuron in the mice would be comprised between 0.74 and 2.67 h (Crowe et al., 2018). However, our data showing that extracellular striatal DA increases as early as 20 min after administration, seem to suggest that this might not be the preferred route. Transport across the nasal epithelium can also use an extracellular pathway, whereby substances cross the Tight Junctions (TJs) between the nasal epithelium and the lamina propria. From there, they can reach the perineural space and delivered in the cerebrospinal fluid (CSF) and the entire brain. This latter transport is significantly faster than the intracellular transport and is consistent with the time-effect seen in our experiment. In fact, it has been calculated that, with this mechanism, a substance would take about 0.33 h to travel the length of the olfactory nerve (Crowe et al., 2018).

Our observation that, at the lower dose, GCS-DA-SLNs would increase DOPAC levels without significantly modifying DA concentration suggests that at least a fraction of DA is transported via vascular passage and metabolized outside the striatum, leading to increased striatal DOPAC levels. A small amount of DA reaching the striatum would be sufficient to stimulate presynaptic D2 dopaminergic autoreceptors, thereby inhibiting further DA release. This would explain the lack of increase in extracellular concentration following the intranasal administration of the lower dose. Administering the higher dose, on the other hand, markedly increased striatal DA concentration and failed to significantly modify DOPAC levels, producing an effect more similar to that observed with intranasal administration of cocaine or amphetamine (De Souza Silva et al., 1997).

Furthermore, analysis of the DOPAC/DA ratio confirms that intranasally administered GCS-DA-SLNs are able to increase DA concentration in the striatum, exhibiting a clear dose-response effect and a time course consistent with previously published data (De Souza Silva et al., 1997).

It is also important to note, relative to the time course of these effects, that the relatively rapid increase in striatal extracellular DA concentrations following intranasal administration of GCS-DA-SLNs is consistent with the initial burst release detected within the first min, providing a fast onset of action (see Fig. 2).

Di Gioia and al. (2015) reported increased striatal dopamine levels following repeated intranasal administration of DA-loaded GCS/DA-CD nanoparticles into the right nostril. However, it is important to note that the experimental conditions in our study differ substantially from those in Di Gioia et al. In fact, in the Di Gioia et al. paper, DA levels were quantified in tissue homogenates, whereas in our study striatal DA was measured *in vivo* as extracellular concentrations using microdialysis. These two approaches capture different neurochemical parameters, and this methodological difference may account for the lack of effect observed by Di Gioia et al. after acute administration. In addition, in our study, DA was administered bilaterally, and extracellular DA was recorded from the right striatum. Since bilateral administration is expected to minimize ipsilateral–contralateral differences, our design is not directly comparable to the unilateral paradigm used by Di Gioia et al.

Finally, it important to mention that following the intranasal administration of GCS-DA-SLNs, we did not observe any overt behavioral changes other than the physiological arousal associated with the necessary handling.

### 3.3. Effect of intranasal injection of DA-SLNs on HCN-mediated $I_h$ in DLS SPNs

To determine whether the increase in extracellular DA concentrations observed after intranasal administration of GCS-DA-SLNs in the microdialysis experiments could be functionally translated into a DA-mediated modulatory action at the level of some neuronal mechanisms, we decided to perform electrophysiological experiments to record $I_h$ currents mediated by hyperpolarization-activated cyclic nucleotide-gated (HCN) channels. In fact, the cytosolic increase of cyclic nucleotides such as cAMP, which can be induced by the activation of $G_s$ protein-coupled receptors such as D1 dopamine receptors, modulates the function of HCN channels (DiFrancesco and Tortora, 1991). Accordingly, several studies have reported that DA increases HCN-mediated $I_h$ amplitude by acting through dopamine D1 receptors in different brain regions, such as the entorhinal cortex (Rosenkranz and Johnston, 2006) and the CA3 field of the hippocampus (Licheri et al., 2023). Although HCN channels are expressed in SPNs of the striatum (Notomi and Shigemoto, 2004; Peng et al., 2023), despite our best efforts, we could not find any previous studies that explicitly report the modulatory effect of DA. Therefore, it was crucial in the present study to first demonstrate that DA bath perfusion of slices regulates $I_h$ in these neurons, and that this action likely originates from its interaction with D1 receptors.

Accordingly, under our experimental conditions, bath perfusion with 2.5 μM DA for 5 min produced a significant ($p < 0.05$) increase in the $I_h$ amplitude recorded in SPNs in response to hyperpolarizing membrane voltage steps (Fig. 4A and B). Two-way ANOVA revealed a significant effect of hyperpolarizing steps [$F(4, 48) = 56.56$, $p = 0.0001$], a significant effect of DA treatment [$F(1, 12) = 8.852$, $p = 0.0116$], and a significant interaction between factors [$F(4, 48) = 3.160$, $p = 0.022$]. Similarly, 5 min bath perfusion with the selective D1 receptor agonist SKF81297 (5 μM) elicited an even greater enhancement of $I_h$ amplitude (Fig. 4C and D). Two-way ANOVA revealed a significant effect of

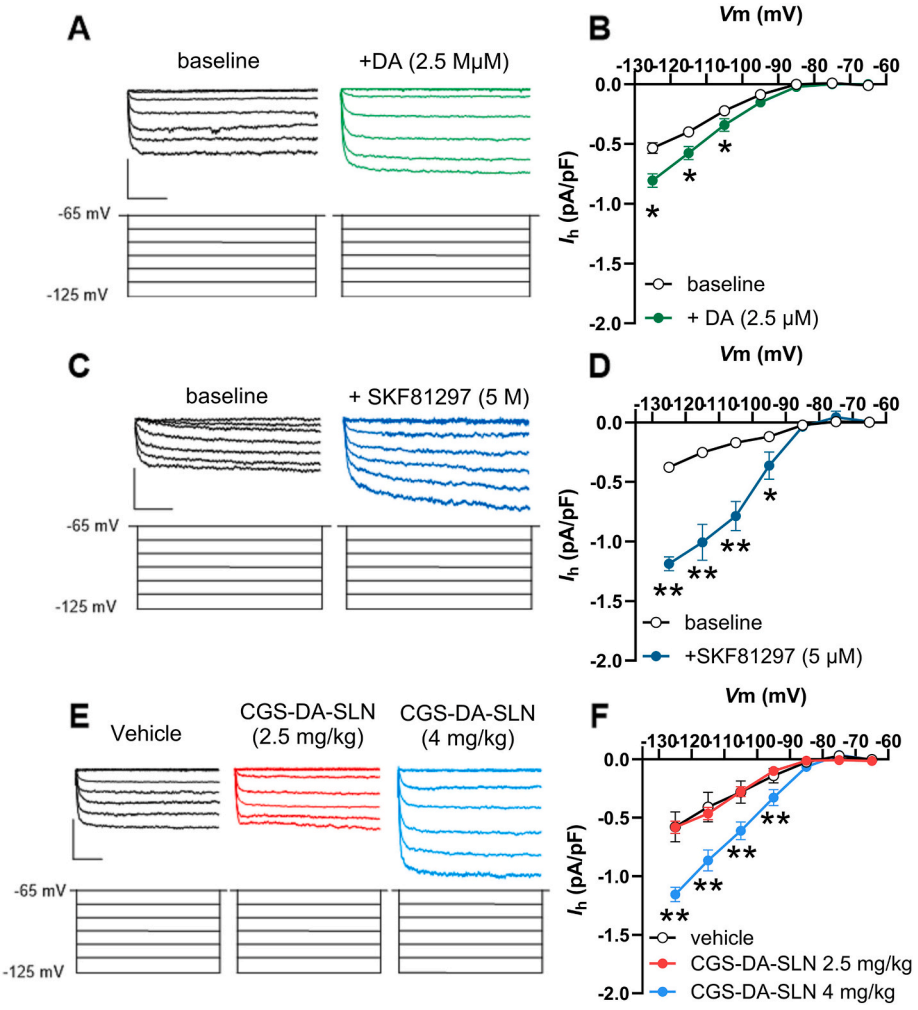


**Fig. 4. Intranasal administration of GCS-DA-SLNs, as well as in vitro dopamine (DA) and the D1 agonist SKF81297, alters HCN-mediated $I_h$ in rat striatal projecting neurons (SPNs).** (**A** and **C**) Representative $I_h$ traces evoked by 1-s steps in membrane hyperpolarization from −65 to −125 mV, obtained *in vitro* from a single DLS spiny neuron before and after 5 min of perfusion with either dopamine (DA) or SKF81297. Scale bar: 100 pA/200 ms. **(B** and **D)** The activation curve of $I_h$ is shown before and after 5 min of bath perfusion with either DA (B) or SKF81297 (D). Data derived from experiments as in A and C are expressed as $I_h$ amplitude normalized to cell capacitance and averaged from 8 (B) and 3 (D) different neurons, ±SEM. *P = 0.05 vs. baseline; **P = 0.001 vs. baseline. **E)** Representative $I_h$ traces recorded in a single rat's striatal spiny neurons in response to increasing membrane hyperpolarization from a holding potential of −65 mV to −125 mV. For this ex vivo experiment, the rats were sacrificed 30 min after receiving GCS-DA-SLNs at corresponding doses of 2.5 or 4 mg/kg of DA or vehicle via intranasal administration. Scale bar: 100 pA/200 ms. **F)** The activation curves of $I_h$ in rat DLM spiny neurons were derived from recordings like those shown in (E). The data are expressed as $I_h$ amplitude (pA), normalized to cell capacitance (pF), and are the average ± SEM, calculated from 8 neurons obtained from 3 rats treated with vehicle; 9 neurons obtained from 3 rats treated with GCS-DA-SLNs at 2.5 mg/kg DA; and 5 neurons obtained from 3 rats treated with GCS-DA-SLNs at 4 mg/kg DA. **P = 0.0001 vs. vehicle.

hyperpolarizing membrane voltage [F (2,386, 9545) = 52.63, p = 0.0001], a significant effect of drug treatment [F (1, 4) = 54.78, p = 0.002], and a significant interaction between the factors [F (4, 16) = 23.26, p = 0.0001].

In the ex vivo experiments, brain slices containing the DLS were obtained from rats sacrificed 30 min after intranasal administration of GCS-DA-SLNs at DA concentrations of 2.5 and 4 mg/kg. This time interval was chosen based on the occurrence of the maximum peak of DA in the microdialysis study (Fig. 3). The results, shown in Fig. 4E and F, indicate that while the $I_h$ amplitude was not altered in rats treated with CGS-DA-SLNs at the dose of 2.5 mg/kg, a positive effect was detected in SPNs obtained from rats treated with CGS-DA-SLNs at the dose of 4 mg/kg. Two-way ANOVA revealed a significant effect of hyperpolarizing membrane voltage [F (6, 133) = 67,80, p = 0.0001], a significant effect of drug treatment only for the dose of 4 mg/kg [F (2, 133) = 23,06, p = 0.0001], and a significant interaction between the factors [F (12, 133) = 3,636, p = 0.0001].

DA and the HCN-mediated hyperpolarization-activated cation current ($I_h$) have a well-established functional interplay, as recently reviewed by Soti et al. (2022). This relationship is particularly relevant in DA neurons and other neuronal populations where DA is able to modulate membrane excitability. The HCN-mediated $I_h$, characterized by its slow activation upon hyperpolarization, contributes critically to pacemaker activity and neuronal excitability (Chu and Zhen, 2010). DA indirectly modulates $I_h$ by altering several channel properties, including its amplitude- and voltage-dependent activation properties. This regulatory action of DA on HCN channels is exerted by intracellular cyclic nucleotides such as cyclic AMP (cAMP) (Chen et al., 2001; DiFrancesco and Tortora, 1991; Santoro et al., 1998), whose cytosolic concentrations can increase as a consequence of selective activation of dopamine D1 receptors (Licheri et al., 2023; Rosenkranz and Johnston, 2006).

Accordingly, the present study showed that both DA and the selective dopamine D1 receptor agonist SKF81297 similarly increased $I_h$ amplitude with no apparent alteration in the voltage-dependent activation of the HCN channel under the experimental conditions employed. In accordance with these findings, our ex vivo electrophysiological experiments demonstrate that intranasal administration of GCS-DA-SLNs at DA concentrations of 4 mg/kg DA, but not 2.5 mg/kg, significantly increases the amplitude of $I_h$ currents in medium striatal neurons (MSNs) of the dorsolateral striatum (DLS) compared to control rats treated with vehicle, in which striatal DA concentrations were not altered as detected in the microdialysis experiment. The present finding indicates with a high degree of probability that the intranasal delivery of GCS-DA-SLNs resulted in the achievement of a pharmacologically active concentration of DA in the DLS, sufficient to activate dopamine D1 receptors and modulate HCN channel-mediated $I_h$ currents.

In contrast, the intranasal administration of GCS-DA-SLNs at DA concentrations of 2.5 mg/kg did not alter $I_h$ amplitude, despite the significant increase in striatal DA concentration. It is probable that lower striatal DA levels may bind predominantly to dopamine D2 receptors which are predominantly in the high-affinity agonist state, making them more responsive to DA (Richfield et al., 1989). Indeed, DA D2 activation, which leads to a lowering in intracellular cAMP concentrations, was reported to reduce $I_h$ amplitude and shift its activation to more hyperpolarized potentials in mouse olfactory receptor neurons, thereby modulating excitability and firing patterns differently (Vargas and Lucero, 1999). It can be hypothesized that the absence of modulatory effects on $I_h$ amplitude subsequent to intranasal administration of the lower dose of GCS-DA-SLNs may thus be attributable to an opposing effect on both subtypes of DA receptors.

It is also important to recognize that our electrophysiological approach has limitations in terms of its ability to detect striatal DA, given all the experimental steps, including time for slice incubation, stabilization and aCSF perfusion during time of recordings, added to the physiologic presence of DA transporters and enzymes. Therefore, we cannot currently demonstrate the direct effect of DA delivered through GCS-DA-SLNs on HCN-mediated $I_h$ currents, but we can infer its modulatory effect by comparing it with the effect of perfusing DA or SKF81297 directly to the slices. However, it should also be noted that *in vitro* DA release indicates that, after an initial burst of DA release consistent with a rapid onset of action (see Fig. 2A), sustained DA release is detected for several hours (Fig. 2B). Additionally, microdialysis experiments show that the time course of DA detection in the striatum of rats administered with GCS-DA-SLNs intranasally at a dose of 4 mg/kg of DA exhibits an increase that peaks at 30 min post-administration and remains significant after 80 min, persisting at these levels. This is much less evident for the 2.5 mg/kg dose of DA, which was ineffective in the electrophysiological experiments. Furthermore, although this was not tested in the present study, our previous research with rat hippocampal slices (Licheri et al., 2023) revealed that applying DA for 5 min produced a prolonged increase in $I_h$ amplitude. The maximum value was reached after 15 min and persisted well beyond the presence of DA in the perfusion bath (up to 40 min). Thus, the sustained release of DA from the nanoparticles, the time course of the increase in striatal DA and the prolonged modulatory effect of DA on $I_h$ may be contributing factors that enabled us to detect changes in ex vivo slice experiments.

Overall, our data underscores the significant potential of employing GCS coated nanocarriers as an efficient system for delivering DA and other therapeutic compounds by utilizing the nose-to-brain pathway. In this respect, it is important to consider the significant anatomical differences existing between rodent and human nasal cavities. In rodents, the olfactory region occupies a much larger proportion of the nasal cavity (up to 40–50 %) compared to less than 10 % in humans, where it is confined to the roof of the nasal cavity and is less accessible for drug deposition (Erdo et al., 2018; Flamm et al., 2021). The respiratory region, which is the main target for systemic drug absorption, covers about 90 % of the nasal cavity in humans but only about 50 % in rodents. Rodent nasal cavities are also narrower and more complex, making precise targeting and reproducibility of drug delivery more challenging, and increasing the risk of unintended swallowing or inhalation during administration (Maigler et al., 2021). These anatomical differences mean that drugs administered intranasally in rodents are more likely to reach the olfactory mucosa and thus the brain, whereas in humans, limited olfactory surface area and accessibility can reduce the efficiency of nose-to-brain delivery (Erdo et al., 2018; Flamm et al., 2021; Keller et al., 2022). Consequently, dosing volumes, administration techniques, and device designs must be carefully adapted when translating findings from rodent models to human clinical applications.

Finally, it is noteworthy that, to the best of our knowledge, this is the first report on nose-to-brain delivery of DA encapsulated in SLNs measuring the neurotransmitter concentration in brain extracellular fluid (brain-ECF) by *in vivo* microdialysis. The usefulness in nose-to-brain delivery of microdialysis evaluations has been already showed using both polymeric nanoparticulate systems (Trapani et al., 2011) and DA containing codrugs (Denora et al., 2012).

Nevertheless, the paper by Ortega Martinez et al. (Ortega Martinez et al., 2024), describing the development of a promising DA formulation based on CS-coated SLNs using glycerol tripalmitin as lipid matrix, attracted our attention even though no *in vivo* results were reported. Hence, the implications of the Ortega Martinez et al. paper (Ortega Martinez et al., 2024), can be compared with those of the present work analyzing the respective formulation properties only. In this regard, it should be noted that the SLN formulation reported by Ortega Martinez et al. showed a particle size >200 nm, unlike that of the present work (Ortega Martinez et al., 2024). This size feature is not advantageous for nanoparticle transport through the olfactory neuronal pathway. Moreover, the E.E.% of neurotransmitter in GCS-DA-SLNs exceeded 80 % compared with 36.3 ± 5.4 % of Ortega Martinez et al. (Ortega Martinez et al., 2024), demonstrating the superior drug encapsulation capability of the former SLNs, probably due to the self-emulsifying properties of the lipid matrix used (i.e., Gelucire® 50/13) combined with GCS coating (Trapani et al., 2021a). From a physical stability point of view both two

nanoparticle types showed similar features being able to maintain good properties only if kept at 4 °C.

## 4. Conclusions

The present study describes the development and characteristics of GCS-DA-SLNs endowed with relevant mucoadhesive properties, diffusion controlled sustained release of the neurotransmitter and demonstrates the efficacy of their intranasal administration in delivering DA to the rat striatum. Intranasal GCS-DA-SLNs resulted in a significant increase in striatal extracellular DA levels and a subsequent modulatory influence on neuronal function. These findings suggest a novel therapeutic approach for neurological conditions characterized by dopaminergic dysfunction, including Parkinson's disease. The intranasal route has been demonstrated to be a non-invasive and potentially more effective method of DA delivery in comparison to traditional systemic approaches. This approach circumvents the BBB, thereby facilitating targeted striatal effects. The microdialysis data and the observed effect on HCN channel function indicates the potential of GCS-DA-SLNs to release DA *in vivo* at concentrations that are sufficient to significantly interact with DA D1-like receptors. This finding suggests that the delivery of sufficient DA to the brain is facilitated by such a system. The delivery of DA occurred with a relatively rapid kinetic; while the sudden increase in DA observed after administration could be useful to rapidly alleviate symptoms associated with neurological disorders, the equally fast return of DA extracellular concentration to basal values makes this route of administration not suitable to guarantee a long-term effect. Following further exploration into the precise electrophysiological and behavioral consequences of this targeted DA delivery, intranasal GCS-DA-SLNs could be considered as an add-on therapy to ensure a rapid response. Further research is warranted to investigate the long-term effects, optimal dosage, and potential side effects of this intranasal SLN delivery system. The potential for enhanced patient compliance and mitigated systemic adverse effects renders this a promising avenue for future therapeutic development.

## CRediT authorship contribution statement

**Laura Dazzi:** Writing – original draft, Investigation, Data curation. **Giuseppe Talani:** Writing – original draft, Investigation, Data curation. **Giuseppe Trapani:** Data curation. **Luigi Capasso:** Investigation. **Annalucia Carbone:** Investigation. **Sante Di Gioia:** Writing – original draft, Data curation. **Massimo Conese:** Writing – review & editing, Writing – original draft. **Adriana Trapani:** Writing – review & editing, Writing – original draft, Supervision, Project administration, Investigation, Funding acquisition, Data curation, Conceptualization. **Enrico Sanna:** Writing – original draft, Funding acquisition, Data curation, Conceptualization.

## Funding

The work presented was supported by Faculty Research Founding to E.S, L.D. and A.T.

## Declaration of competing interest

The authors have no competing interests to declare that are relevant to the content of this article.

## Acknowledgments

A.T. would acknowledge Dr. Philippe Caisse (Gattefossè, France) for providing the lipid Gelucire® 50/13, Dr. Silvia D′ Eusebio and Mr. Sergio Cellamare (University of Bari, Italy) for their valuable technical assistance.

## Data availability

Data will be made available on request.

## References

Adermark, L., Talani, G., Lovinger, D.M., 2009. Endocannabinoid-dependent plasticity at GABAergic and glutamatergic synapses in the striatum is regulated by synaptic activity. Eur. J. Neurosci. 29, 32–41.

Bourganis, V., Kammona, O., Alexopoulos, A., Kiparissides, C., 2018. Recent advances in carrier mediated nose-to-brain delivery of pharmaceutics. Eur. J. Pharm. Biopharm. 128, 337–362.

Buddenberg, T.E., Topic, B., Mahlberg, E.D., de Souza Silva, M.A., Huston, J.P., Mattern, C., 2008. Behavioral actions of intranasal application of dopamine: effects on forced swimming, elevated plus-maze and open field parameters. Neuropsychobiology 57, 70–79.

Cassano, R., Trapani, A., Di Gioia, M.L., Mandracchia, D., Pellitteri, R., Tripodo, G., Trombino, S., Di Gioia, S., Conese, M., 2020. Synthesis and characterization of novel chitosan-dopamine or chitosan-tyrosine conjugates for potential nose-to-brain delivery. Int. J. Pharm. 589, 119829.

Castellani, S., Iaconisi, G.N., Tripaldi, F., Porcelli, V., Trapani, A., Messina, E., Guerra, L., Di Franco, C., Maruccio, G., Monteduro, A.G., Corbo, F., Di Gioia, S., Trapani, G., Conese, M., 2024. Dopamine and Citicoline-Co-Loaded solid lipid nanoparticles as multifunctional nanomedicines for Parkinson's Disease treatment by intranasal administration. Pharmaceutics 16.

Cerri, S., Mus, L., Blandini, F., 2019. Parkinson's Disease in women and men: what's the difference? J. Parkinsons Dis. 9, 501–515.

Chao, O.Y., Mattern, C., Silva, A.M., Wessler, J., Ruocco, L.A., Nikolaus, S., Huston, J.P., Pum, M.E., 2012. Intranasally applied L-DOPA alleviates parkinsonian symptoms in rats with unilateral nigro-striatal 6-OHDA lesions. Brain Res. Bull. 87, 340–345.

Chemuturi, N.V., Donovan, M.D., 2006. Metabolism of dopamine by the nasal mucosa. J. Pharmacol. Sci. 95, 2507–2515.

Chemuturi, N.V., Haraldsson, J.E., Prisinzano, T., Donovan, M., 2006. Role of dopamine transporter (DAT) in dopamine transport across the nasal mucosa. Life Sci. 79, 1391–1398.

Chen, S., Wang, J., Siegelbaum, S.A., 2001. Properties of hyperpolarization-activated pacemaker current defined by coassembly of HCN1 and HCN2 subunits and basal modulation by cyclic nucleotide. J. Gen. Physiol. 117, 491–504.

Chu, H.Y., Zhen, X., 2010. Hyperpolarization-activated, cyclic nucleotide-gated (HCN) channels in the regulation of midbrain dopamine systems. Acta Pharmacol. Sin. 31, 1036–1043.

Cometa, S., Bonifacio, M.A., Trapani, G., Di Gioia, S., Dazzi, L., De Giglio, E., Trapani, A., 2020. In vitro investigations on dopamine loaded solid lipid nanoparticles. J. Pharm. Biomed. Anal. 185, 113257.

Crowe, T.P., Greenlee, M.H.W., Kanthasamy, A.G., Hsu, W.H., 2018. Mechanism of intranasal drug delivery directly to the brain. Life Sci. 195, 44–52.

Crowe, T.P., Hsu, W.H., 2022. Evaluation of recent intranasal drug delivery systems to the central nervous system. Pharmaceutics 14, 629.

Dahlin, M., Bergman, U., Jansson, B., Bjork, E., Brittebo, E., 2000. Transfer of dopamine in the olfactory pathway following nasal administration in mice. Pharm. Res. 17, 737–742.

Dazzi, L., Serra, M., Seu, E., Cherchi, G., Pisu, M.G., Purdy, R.H., Biggio, G., 2002. Progesterone enhances ethanol-induced modulation of mesocortical dopamine neurons: antagonism by finasteride. J. Neurochem. 83, 1103–1109.

De Giglio, E., Bakowsky, U., Engelhardt, K., Caponio, A., La Pietra, M., Cometa, S., Castellani, S., Guerra, L., Fracchiolla, G., Poeta, M.L., Mallamaci, R., Cardone, R.A., Bellucci, S., Trapani, A., 2023. Solid lipid nanoparticles containing dopamine and grape seed extract: freeze-drying with cryoprotection as a formulation strategy to achieve nasal powders. Molecules 28, 7706.

De Souza Silva, M.A., Mattern, C., Hacker, R., Nogueira, P.J., Huston, J.P., Schwarting, R. K., 1997. Intranasal administration of the dopaminergic agonists L-DOPA, amphetamine, and cocaine increases dopamine activity in the neostriatum: a microdialysis study in the rat. J. Neurochem. 68, 233–239.

de Souza Silva, M.A., Topic, B., Huston, J.P., Mattern, C., 2008. Intranasal dopamine application increases dopaminergic activity in the neostriatum and nucleus accumbens and enhances motor activity in the open field. Synapse 62, 176–184.

Denora, N., Cassano, T., Laquintana, V., Lopalco, A., Trapani, A., Cimmino, C.S., Laconca, L., Giuffrida, A., Trapani, G., 2012. Novel codrugs with GABAergic activity for dopamine delivery in the brain. Int. J. Pharm. 437, 221–231.

Di Gioia, S., Trapani, A., Mandracchia, D., De Giglio, E., Cometa, S., Mangini, V., Arnesano, F., Belgiovine, G., Castellani, S., Pace, L., Lavecchia, M.A., Trapani, G., Conese, M., Puglisi, G., Cassano, T., 2015. Intranasal delivery of dopamine to the striatum using glycol chitosan/sulfobutylether-beta-cyclodextrin based nanoparticles. Eur. J. Pharm. Biopharm. 94, 180–193.

DiFrancesco, D., Tortora, P., 1991. Direct activation of cardiac pacemaker channels by intracellular cyclic AMP. Nature 351, 145–147.

Erdo, F., Bors, L.A., Farkas, D., Bajza, A., Gizurarson, S., 2018. Evaluation of intranasal delivery route of drug administration for brain targeting. Brain Res. Bull. 143, 155–170.

Flamm, J., Hartung, S., Ganger, S., Maigler, F., Pitzer, C., Schindowski, K., 2021. Establishment of an olfactory region-specific intranasal delivery technique in mice to target the central nervous system. Front. Pharmacol. 12, 789780.

Gandhi, S., Shastri, D.H., Shah, J., Nair, A.B., Jacob, S., 2024. Nasal delivery to the brain: harnessing nanoparticles for effective drug transport. Pharmaceutics 16.

Hayes, M.T., 2019. Parkinson's disease and parkinsonism. Am. J. Med. 132, 802–807.
Keller, L.A., Merkel, O., Popp, A., 2022. Intranasal drug delivery: opportunities and toxicologic challenges during drug development. Drug Deliv Transl Res 12, 735–757.
Licheri, V., Talani, G., Biggio, G., Sanna, E., 2023. Bi-directional modulation of hyperpolarization-activated cation currents (I(h)) by ethanol in rat hippocampal CA3 pyramidal neurons. Neuropharmacology 227, 109423.
Lofts, A., Abu-Hijleh, F., Rigg, N., Mishra, R.K., Hoare, T., 2022. Using the intranasal route to administer drugs to treat neurological and psychiatric illnesses: Rationale, successes, and future needs. CNS Drugs 36, 739–770.
Maigler, F., Ladel, S., Flamm, J., Ganger, S., Kurpiers, B., Kiderlen, S., Volk, R., Hamp, C., Hartung, S., Spiegel, S., Soleimanizadeh, A., Eberle, K., Hermann, R., Krainer, L., Pitzer, C., Schindowski, K., 2021. Selective CNS targeting and distribution with a refined region-specific intranasal delivery technique via the olfactory mucosa. Pharmaceutics 13, 1904.
Mallamaci, R., Musaro, D., Greco, M., Caponio, A., Castellani, S., Munir, A., Guerra, L., Damato, M., Fracchiolla, G., Coppola, C., Cardone, R.A., Rashidi, M., Tardugno, R., Sergio, S., Trapani, A., Maffia, M., 2024. Dopamine- and grape-seed-extract-loaded solid lipid nanoparticles: interaction studies between particles and differentiated SH-SY5Y neuronal cell model of parkinson's disease. Molecules 29.
Muddapu, V.R., Chakravarthy, V.S., 2021. Influence of energy deficiency on the subcellular processes of substantia nigra pars compacta cell for understanding Parkinsonian neurodegeneration. Sci. Rep. 11, 1754.
Mura, P., Maestrelli, F., D'Ambrosio, M., Luceri, C., Cirri, M., 2021. Evaluation and comparison of solid lipid nanoparticles (SLNs) and nanostructured lipid carriers (NLCs) as vectors to develop hydrochlorothiazide effective and safe pediatric oral liquid formulations. Pharmaceutics 13.
Notomi, T., Shigemoto, R., 2004. Immunohistochemical localization of Ih channel subunits, HCN1-4, in the rat brain. J. Comp. Neurol. 471, 241–276.
Ortega Martinez, E., Morales Hernandez, M.E., Castillo-Gonzalez, J., Gonzalez-Rey, E., Ruiz Martinez, M.A., 2024. Dopamine-loaded chitosan-coated solid lipid nanoparticles as a promise nanocarriers to the CNS. Neuropharmacology 249, 109871.
Palazzo, C., Trapani, G., Ponchel, G., Trapani, A., Vauthier, C., 2017. Mucoadhesive properties of low molecular weight chitosan- or glycol chitosan- and corresponding thiomer-coated poly(isobutylcyanoacrylate) core-shell nanoparticles. Eur. J. Pharm. Biopharm. 117, 315–323.
Paxinos, G., Watson, C., 2004. The Rat Brain in Stereotaxic Coordinates - the New Coronal Set. Academic Press, New York.
Peng, J.Y., Qi, Z.X., Yan, Q., Fan, X.J., Shen, K.L., Huang, H.W., Lu, J.H., Wang, X.Q., Fang, X.X., Mao, L., Ni, J., Chen, L., Zhuang, Q.X., 2023. Ameliorating parkinsonian motor dysfunction by targeting histamine receptors in entopeduncular nucleus-thalamus circuitry. Proc. Natl. Acad. Sci. U. S. A. 120, e2216247120.
Pum, M.E., Schable, S., Harooni, H.E., Topic, B., De Souza Silva, M.A., Li, J.S., Huston, J. P., Mattern, C., 2009. Effects of intranasally applied dopamine on behavioral asymmetries in rats with unilateral 6-hydroxydopamine lesions of the nigro-striatal tract. Neuroscience 162, 174–183.
Rehman, S., Nabi, B., Zafar, A., Baboota, S., Ali, J., 2019. Intranasal delivery of mucoadhesive nanocarriers: a viable option for Parkinson's disease treatment? Expet Opin. Drug Deliv. 16, 1355–1366.
Richfield, E.K., Penney, J.B., Young, A.B., 1989. Anatomical and affinity state comparisons between dopamine D1 and D2 receptors in the rat central nervous system. Neuroscience 30, 767–777.
Rosenkranz, J.A., Johnston, D., 2006. Dopaminergic regulation of neuronal excitability through modulation of Ih in layer V entorhinal cortex. J. Neurosci. 26, 3229–3244.
Saha, P., Kathuria, H., Pandey, M.M., 2023. Intranasal nanotherapeutics for brain targeting and clinical studies in Parkinson's disease. J. Contr. Release 358, 293–318.
Santoro, B., Liu, D.T., Yao, H., Bartsch, D., Kandel, E.R., Siegelbaum, S.A., Tibbs, G.R., 1998. Identification of a gene encoding a hyperpolarization-activated pacemaker channel of brain. Cell 93, 717–729.
Soti, M., Ranjbar, H., Kohlmeier, K.A., Razavinasab, M., Masoumi-Ardakani, Y., Shabani, M., 2022. Probable role of the hyperpolarization-activated current in the dual effects of CB1R antagonism on behaviors in a Parkinsonism mouse model. Brain Res. Bull. 191, 78–92.
Trapani, A., De Giglio, E., Cafagna, D., Denora, N., Agrimi, G., Cassano, T., Gaetani, S., Cuomo, V., Trapani, G., 2011. Characterization and evaluation of chitosan nanoparticles for dopamine brain delivery. Int. J. Pharm. 419, 296–307.
Trapani, A., De Giglio, E., Cometa, S., Bonifacio, M.A., Dazzi, L., Di Gioia, S., Hossain, M. N., Pellitteri, R., Antimisiaris, S.G., Conese, M., 2021a. Dopamine-loaded lipid based nanocarriers for intranasal administration of the neurotransmitter: a comparative study. Eur. J. Pharm. Biopharm. 167, 189–200.
Trapani, A., Guerra, L., Corbo, F., Castellani, S., Sanna, E., Capobianco, L., Monteduro, A. G., Manno, D.E., Mandracchia, D., Di Gioia, S., Conese, M., 2021b. Cyto/Biocompatibility of dopamine combined with the antioxidant grape seed-derived polyphenol compounds in solid lipid nanoparticles. Molecules 26, 916.
Trapani, A., Mandracchia, D., Di Franco, C., Cordero, H., Morcillo, P., Comparelli, R., Cuesta, A., Esteban, M.A., 2015. In vitro characterization of 6-Coumarin loaded solid lipid nanoparticles and their uptake by immunocompetent fish cells. Colloids Surf. B Biointerfaces 127, 79–88.
Trapani, A., Palazzo, C., Contino, M., Perrone, M.G., Cioffi, N., Ditaranto, N., Colabufo, N.A., Conese, M., Trapani, G., Puglisi, G., 2014. Mucoadhesive properties and interaction with P-glycoprotein (P-gp) of thiolated-chitosans and -glycol chitosans and corresponding parent polymers: a comparative study. Biomacromolecules 15, 882–893.
Turner, P.V., Pekow, C., Vasbinder, M.A., Brabb, T., 2011. Administration of substances to laboratory animals: equipment considerations, vehicle selection, and solute preparation. J Am Assoc Lab Anim Sci 50, 614–627.
Uchino, H., Kanai, Y., Kim, D.K., Wempe, M.F., Chairoungdua, A., Morimoto, E., Anders, M.W., Endou, H., 2002. Transport of amino acid-related compounds mediated by L-type amino acid transporter 1 (LAT1): insights into the mechanisms of substrate recognition. Mol. Pharmacol. 61, 729–737.
Umek, N., Geršak, B., Vintar, N., Šoštarič, M., Mavrim, J., 2018. Dopamine autoxidation is controlled by acidic pH. Front. Mol. Neurosci. 11, 467, 2018 Dec 18.
Vargas, G., Lucero, M.T., 1999. Dopamine modulates inwardly rectifying hyperpolarization-activated current (Ih) in cultured rat olfactory receptor neurons. J. Neurophysiol. 81, 149–158.
Zheng, Y., Cui, L., Lu, H., Liu, Z., Zhai, Z., Wang, H., Shao, L., Lu, Z., Song, X., Zhang, Y., 2024. Nose to brain: exploring the progress of intranasal delivery of solid lipid nanoparticles and nanostructured lipid carriers. Int. J. Nanomed. 19, 12343–12368.